NASA CR- 163,593

HANDLING QUALITIES OF LARGE FLEXIBLE AIRCRAFT

NASA-CR-163593

By

SUPAT POOPAKA

Bachelor of Science
Prince of Songkla University
Haadyai, Thailand
1972

Master of Science
University of Illinois
Urbana, Illinois
1977

Submitted to the Faculty of the
Graduate College of the
Oklahoma State University
in partial fulfillment of
the requirements for
the Degree of
DOCTOR OF PHILOSOPHY
December 1980

Name: Supat Poopaka   Date of Degree: December, 1980

Institution: Oklahoma State University Location: Stillwater, Oklahoma

Title of Study: HANDLING QUALITIES OF LARGE FLEXIBLE AIRCRAFT

Pages in Study: 61   Candidate for Degree of Doctor of Philosophy

Major Field: Mechanical Engineering

Scope and Method of Study: The effects on handling qualities of elastic
    modes interaction with the rigid body dynamics of a large flexible
    aircraft are studied by a mathematical computer simulation. An
    analytical method to predict the pilot ratings when there is a se-
    vere modes interaction is developed. This is done by extending the
    optimal control model of the human pilot response to include the
    mode decomposition mechanism into the model. The handling quali-
    ties are determined for a longitudinal tracking task using a large
    flexible aircraft with parametric variations in the undamped nat-
    ural frequencies of the two lowest frequency, symmetric elastic
   modes made to induce varying amounts of mode interaction.

Findings and Conclusions: The modified model of the human pilot re-
    sponse developed in this study proved successful in descriminating
    when the pilot can or cannot separate rigid from elastic response
    in the tracking task. A comparison of the model predictions with
    the past experimental data shows that the modified pilot model is
    much better in predicting the elastic modes interaction effect on
    the handling qualities than the standard optimal control model of
    the human pilot. The techniques developed here make it easier to
    investigate the effects of elastic modes interaction with the rig-
    id body dynamics of a large flexible aircraft on the handling
    qualities in a preliminary design stage.

ADVISOR'S APPROVAL _____

HANDLING QUALITIES OF LARGE FLEXIBLE AIRCRAFT

Thesis Approved:

_____
Thesis Advisor

_____

_____

_____

_____
Dean of the Graduate College

ACKNOWLEDGMENTS

TABLE OF CONTENTS

LIST OF TABLES

LIST OF FIGURES

A_a — Matrix of physical state coefficients in the vehicle equations of motion

A_g — Gust matrix

a_i — Half width of dead zone element

B_a — Matrix of control variable coefficients in the vehicle equations of motion

b_w — Aircraft wing span

C_a — Matrix of output variable coefficients in the vehicle attitude director equations

$\bar{c}_w$ — Wing mean aerodynamic chord

D_a — Control distribution Matrix for observations

E_a — Matrix of disturbance variable coefficients

$E\{\cdot\}$ — Expected value of $\{\cdot\}$

f_i — Fraction of attention allocated to i^{th} display variable

ft — Feet

G — Scalar white noise coefficient vector in the vehicle equations of motion

g — Local gravitational acceleration (32.17 ft/s^2)

I_y — Mass moment of inertia about stability axis y

J — Cost functional

L_u — Longitudinal gust scale factor

L_w — Vertical gust scale factor

m — Airplane mass

N   - Describing function gain for the threshold element

P.O.R.- Pilot opinion rating in Cooper-Harper scale

Q_r - Weighting on control rate

Q_y - Weighting on display variables

Q_{ξ_i} - Generalized force of the ith elastic mode

q   - Perturbation pitch angle rate (same as $\dot{\theta}$)

q_g - Perturbation of q due to variations in vertical gust properties along the centerline of the vehicle

r   - τ-second delayed of the pilot control input

S_w - Wing area

s   - Second

      - Laplace transform variable

T_n - Neuromuscular constant matrix

t   - time (s)

U_o - Steady state vehicle velocity

u   - Perturbation forward speed

u_a - Control input vector

u_g - Perturbation of u due to gust

u_m - "Commanded" control input

V_m - Motor noise covariance matrix

V_y - Observation noise covariance matrix

v_m - Motor noise

v_y - Observation noise

w_a - Random external disturbance

x_a - State vector associated with the physical output states of the aircraft

y_a - Display information vector

y_p — Perceived display quantities

α — Perturbation angle of attack

α_g — Perturbation of α due to gust

δ_e — Elevator deflection

θ — Perturbation pitch angle

θ_g — Perturbation of θ_g due to gust

ρ_i — Multiplicative noise/signal ratio

σ_i^2 — Noise variance of i

Σ — Error covariance matrix

τ — Perceptual time delay

μ — Small positive parameter which arises due to the presence of of high frequency elastic modes

ω — Temporal frequency in turbulence model

ω_i — In-vacuum elastic mode undamped natural frequency of ith mode

ω_{i_e} — Coupled undamped natural frequency of ith mode

ω_{ph} — Natural frequency of phugoid mode

ω_{sp} — Natural frequency of short-period mode

ζ_i — Structural damping ratio of mode i

ζ_{i_e} — Coupled damping ratio of ith mode

ζ_{ph} — Damping ratio of phugoid mode

ξ_{sp} — Damping ratio of short-period mode

ξ_i — Generalized coordinate of ith elastic mode

ϕ_i' — Slope of ith normalized mode shape

CHAPTER 1

INTRODUCTION

The handling or flying qualities of a piloted aircraft are the static and dynamic characteristics that influence the ease and precision with which a pilot is able to perform the control task required in support of the aircraft mission flight phase. Thus, the handling qualities depend not only on aircraft characteristics and a mission flight phase but also on the pilot's subjective opinion of the ease with which he can perform the control task.

To accurately assess the pilot's opinion of the handling qualities of an aircraft prior to first flight of a prototype, a groundbased simulation is usually required. In the early stages of the design, it is more economical to use a mathematical pilot modeling simulation because the design parameters can be easily adjusted. The pilot's assessment is then related to some scale such as the widely accepted Cooper-Harper pilot rating scale (Figure 1).

Much research has been done to determine the relations between the parameters of the rigid body, small perturbation equations of motion and the pilot rating. The handling qualities requirements for a rigid airplane in Chalk et al. [1] are typical results of such research. Most of the airplanes in the past have been relatively rigid such that the elasticity of the airplanes do not contribute significantly to the pilot perceived handling qualities.

1

ADEQUACY FOR SELECTED TASK OR REQUIRED OPERATION*

AIRCRAFT CHARACTERISTICS * DEMANDS ON THE PILOT IN SELECTED TASK OR REQUIRED OPERATION*

PILOT RATING

Aircraft Characteristics	Demands on the Pilot in Selected Task or Required Operation*	Pilot Rating
Excellent Highly desirable	Pilot compensation not a factor for desired performance	1
Good Negligible deficiencies	Pilot compensation not a factor for desired performance	2
Fair - Some mildly unpleasant deficiencies	Minimal pilot compensation required for desired performance	3
Minor but annoying deficiencies	Desired performance requires moderate pilot compensation	4
Moderately objectionable deficiencies	Adequate performance requires considerable pilot compensation	5
Very objectionable but tolerable deficiencies	Adequate performance requires extensive pilot compensation	6
Major deficiencies	Adequate performance not attainable with maximum tolerable pilot compensation. Controllability not in question	7
Major deficiencies	Considerable pilot compensation is required for control	8
Major deficiencies	Intense pilot compensation is required to retain control	9
Major deficiencies	Control will be lost during some portion of required operation	10

Flowchart (left side):

- Is it satisfactory without improvement? — Yes → (to ratings 1-3) / No → Deficiencies warrant improvement (ratings 4-6)
- Is adequate performance attainable with a tolerable pilot workload? — Yes → / No → Deficiencies require improvement (ratings 7-9)
- Is it controllable? — Yes → / No → Improvement mandatory (rating 10)
- Pilot decisions

*Definition of required operation involves designation of flight phase and/or subphases with accompanying conditions

Figure 1. The Cooper-Harper Pilot Rating Scale [1]

Recent advances in control-configured vehicles design and active control technology makes it possible to increase aircraft size and the utilization of lighter structures in future designs. The elastic behavior of these vehicles is therefore becoming an appreciable influence in their handling qualities. Because of the potential adverse effects of mode interaction with the rigid body dynamics, there is a need for handling qualities assessment in the preliminary design phase of new airplanes.

General Background

It is known that static aeroelastic deflections of an aircraft structure modify the aerodynamic pressure distributions which results in stability derivative changes associated with the rigid body, small perturbation equations of motion. Early attempts to account for aeroelastic effects on aircraft stability and control took the approach of making static aeroelastic corrections to the aerodynamic stability derivatives [2-4]. The drawbacks of this approach as pointed out by Milne [4] are that in calculating modified stability derivatives one is to imagine the major parts of the airplane to be kinematically constrained at various points which do not have any real physical meaning, and if the overall-motion frequencies are of the same order as the lower typical vibration natural frequencies of the structure then the approach is invalid.

For flying in high dynamic pressure environments, such as terrain following in turbulent air, the dynamic effects of flexibility are important enough that they must be included as additional degrees of freedom. A common approach has been to approximate the dynamics by a truncated set of superimposed orthogonal vibration modes. In this case

the phenomena of most interest are the effects of aerodynamic coupling between the various elastic modes and between elastic and rigid body modes, as well as elastic mode interaction with the feedback control system. Reference [5] was one of the earliest comprehensive studies of this problem. The most recent comprehensive work done under the AFFDL sponsorship is documented in reference [6].

The subject of handling qualities requirements and criteria for highly elastic airplanes in turbulent and high dynamic pressure environments has been largely ignored. Much of the research on handling qualities has been concerned with relatively rigid, tactical military aircraft. The handling qualities parameters, such as phugoid, short-period, dutch-roll frequencies and damping ratios, which have been determined pertinent for such airplanes, are mostly meaningless for a flexible airplane with elastic mode frequencies close to the rigid body frequencies. When multiple frequencies are in proximity to one another, the pilot cannot easily discern individual modes of motion; rather his opinion of the transient dynamics will likely be based on the time history of the total motion. No performance criteria suitable for handling qualities specification are presently available for such higher-order responses. This is all too evident in that no useful discussion of aeroelastic effects is included in the revision to the military aircraft handling qualities specification [1]. It contains only the following statement:

> Since aeroelasticity, control equipment, and structural dynamics may exert an important influence on the airplane flying qualities, such effects should not be overlooked in calculations or analysis directed toward investigation of compliance with requirements of this specification (p. 497).

The specification is concerned only with desirable ranges of values on rigid body static and dynamic response parameters. There are methods available for estimating static aeroelastic corrections to rigid body aerodynamic stability derivatives [7]; however, the specification then requires the use of these in rigid aircraft equations of motion. It seems quite possible that the desirable ranges of parameter values could be significantly affected by elastic mode degrees of freedom, particularly when some of the modes have natural frequencies of the same order of magnitudes as the frequencies of the rigid body alone. It is not at all clear that the handling qualities should be specified by rigid body dynamic parameters when such mode interaction is present. In fact, the pilot could not tell, for example, how much of a given pitch angle response to command input is due to rigid body and how much to low frequency elastic modes.

The key in developing handling qualities criteria and eventually specifications for severe mode interaction situations is to establish when and under what conditions the pilot can visually separate the rigid body response from the total response. In conditions when he cannot, a structural mode suppression control system probably will be required.

Objectives and Scope of Study

The primary objective was to develop an analytical method to determine the boundary between when the pilot can visually separate the rigid body motion from the total motion and when he cannot in terms of the small perturbation equations of motion parameters. This study is an extension of the experimental work done in reference [8], where a ground-based pilot-flown simulation was studied. The mathematical

pilot modeling simulation approach is used to assess the effects of mode interaction on the pilot opinion rating.

An extension of the optimal control model for the human pilot [9] is made so that the effects of mode interaction can be assessed. The extension is motivated by an observation of the experimental evidences of reference [8].

Plan of Presentation

A summary of past results is presented in Chapter II. The longitudinal equations of motion for a flexible airplane are developed in Chapter III. The general description and flight condition of the flexible airplane under study are also described in that chapter. Numerical values of stability derivatives for the equations of motion are given in Appendix A. The pilot modeling and its extension is presented in Chapter IV. Derivations of some singular perturbation techniques needed in Chapter IV are summarized in Appendix B. The major results are presented in Chapter V. The conclusions and recommendations appear in Chapter VI.

CHAPTER II

PAST RESULTS

The only research of which we are aware that is directly relevant to the subject is documented in Crother [10] and Yen [8].

The results of North American Rockwell in Crother [10] were for an early version for the B-1 aircraft and included piloted simulator evaluations of tracking performance in turbulence. They concluded that the structural dynamics appeared as essentially a nuisance oscillation to the pilots and did not significantly effect tracking performance. However, the longitudinal dynamics of their configuration were very close to Case 1 of our results. Thus, it is not surprising that the elasticity did not significantly degrade pilot opinion; it was merely a ripple on the rigid body response.

In the work of Yen [8], the effects of parametric lowering of the undamped natural frequencies of the first two symmetric elastic modes of a flexible aircraft were investigated. A pitch tracking task, which included phugoid and short period dynamics, was programmed on a fixed-base simulator with a CRT attitude-director display of pitch command, total pitch angle and pitch error. The display and its variables are depicted in Figures 2 and 3.

The attitude-director equations are

$$\theta_i(x_p, t) = \theta(t) - 0.025\xi_1(t) - 0.029\xi_2(t) \tag{3.1}$$

$$\text{pitch error} = e_\theta = \theta_i - \theta_c \tag{3.2}$$

where 0.025 and 0.029 are the slopes of the two elastic modes at the pilot station. The flight condition is Mach 0.85 at sea level density.

Four pilots each flew eight cases which were combinations of elastic mode interaction. The cases are shown in Table I. Case 1 is the original dynamics. Case 6 was the most difficult, where the free-free elastic mode frequencies were set at 6.93 rad/s for both modes. This resulted in the phugoid mode splitting into positive and negative real roots. Sample time histories of one pilot's tracking difficulty on Case 6 are shown in Figure 4. Note the large amplitudes of the elastic modes' contributions to total pitch θ_i relative to rigid pitch θ. This made it very difficult for the pilot to visually separate rigid from elastic pitch. The average of the four pilots' ratings of Case 6 was 6.7 on the Cooper-Harper scale. Contrast this with a 1.6 rating on Case1, the original dynamics. This work has clearly established the potential seriousness of elastic-rigid body low frequency mode interaction to handling qualities specifications and pilot rating.
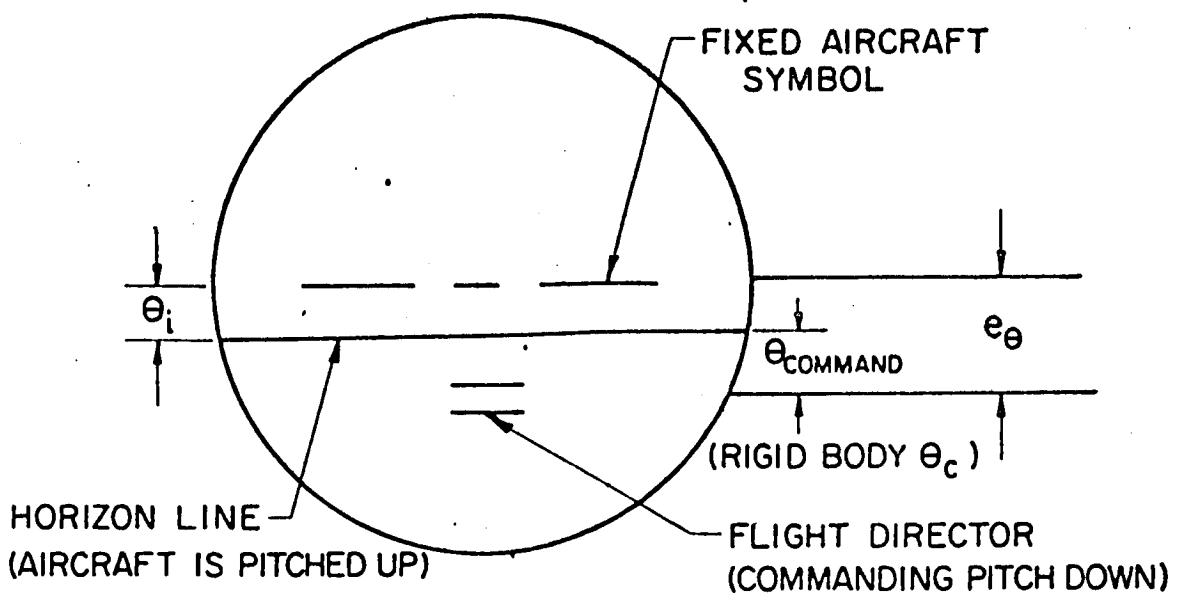
Figure 2. Electronic Attitude Director Indicator (EADI)
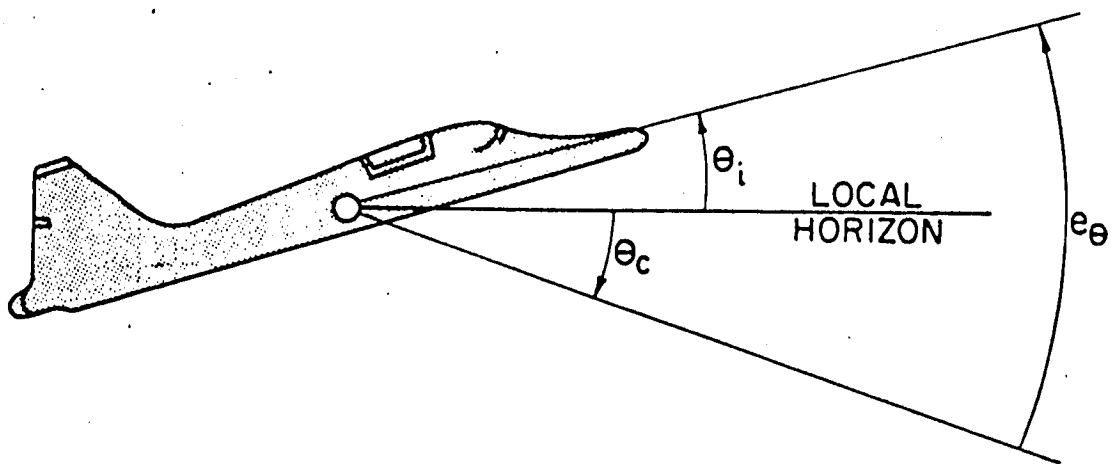
Figure 3. The Airplane Attitude Corresponding To Above EADI

TABLE I

NATURAL FREQUENCIES AND DAMPING RATIOS OF EIGHT CASES

Case #	ω_1 rad/sec	ω_2 rad/sec	ζ_{sp}	ω_{sp} rad/sec	ζ_{ph}	ω_{ph} rad/sec	ζ_{1e}	ω_{1e} rad/sec	ζ_{2e}	ω_{2e} rad/sec	P.O.R.
1	13.59	21.18	0.5339	2.806	0.0197	0.0708	0.0494	13.312	0.0215	21.354	1.6
2	9.17	21.18	0.5235	2.5724	-0.00060267	0.0573	0.08769	8.7891	0.0213	21.356	2.0
3	6.16	21.18	0.5217	1.7691	Real Roots +0.090978 -0.076723		0.1999	5.8669	0.0213	21.357	5.9
4	13.59	4.79	0.6872	1.5745	Real Roots +0.14654 -0.13167		0.05284	13.270	0.1137	5.9702	3.1
5	11.66	11.66	0.5436	2.5819	-0.0001122	0.0537	0.0773	11.801	0.0162	11.574	2.0
6	6.93	6.93	0.7028	1.3665	Real Roots +0.17581 -0.15307		0.1919	7.3305	0.007599	6.9178	6.7
7	10.25	9.75	0.5517	-0.0483		0.0282	0.1129	10.234	-0.0004277	9.8978	2.3
8	10.68	9.27	2.3893	-0.0541		0.0256	0.11021	10.347	0.0005306	9.7781	1.9
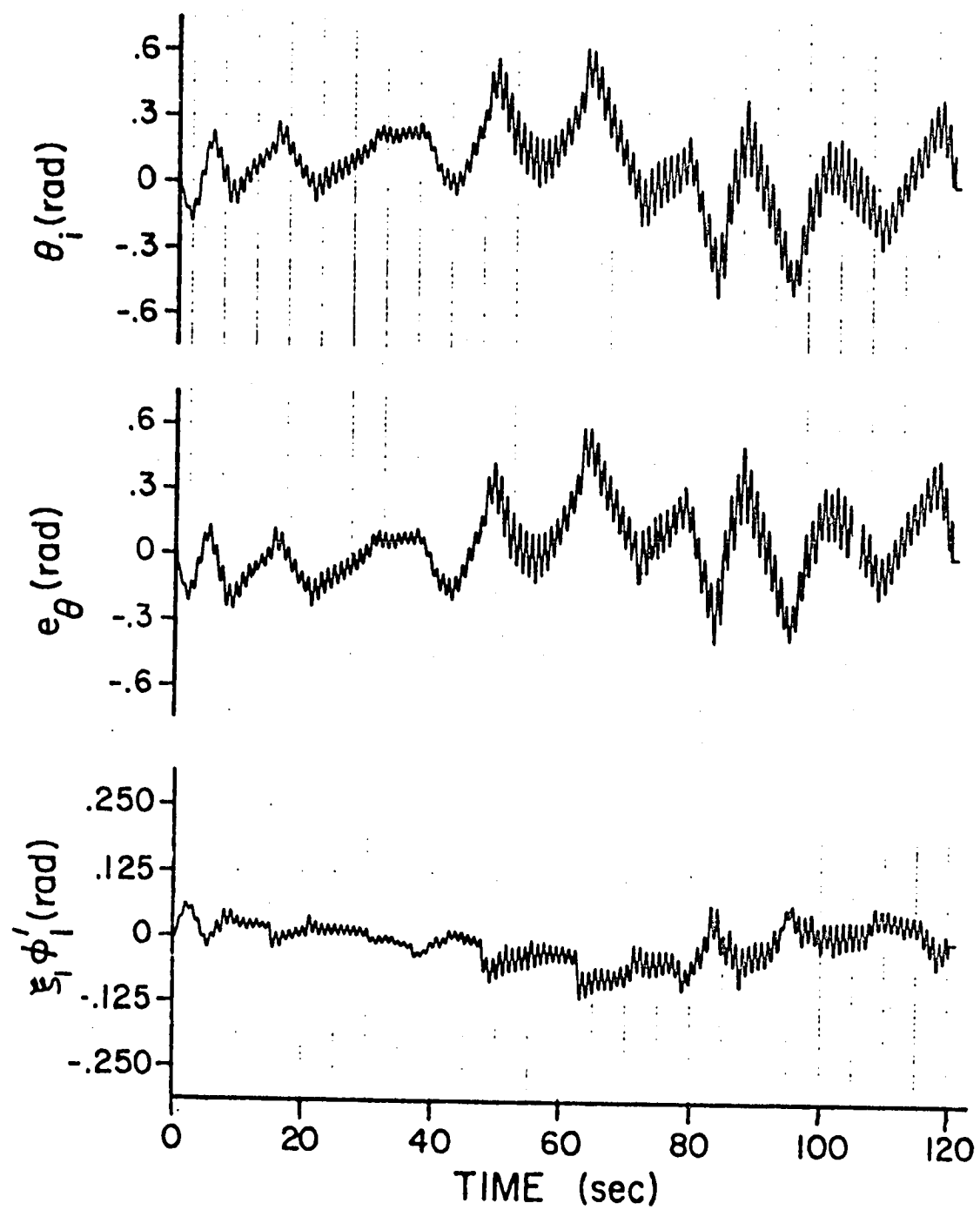
-A-

Figure 4. Sample Time History-Case 6
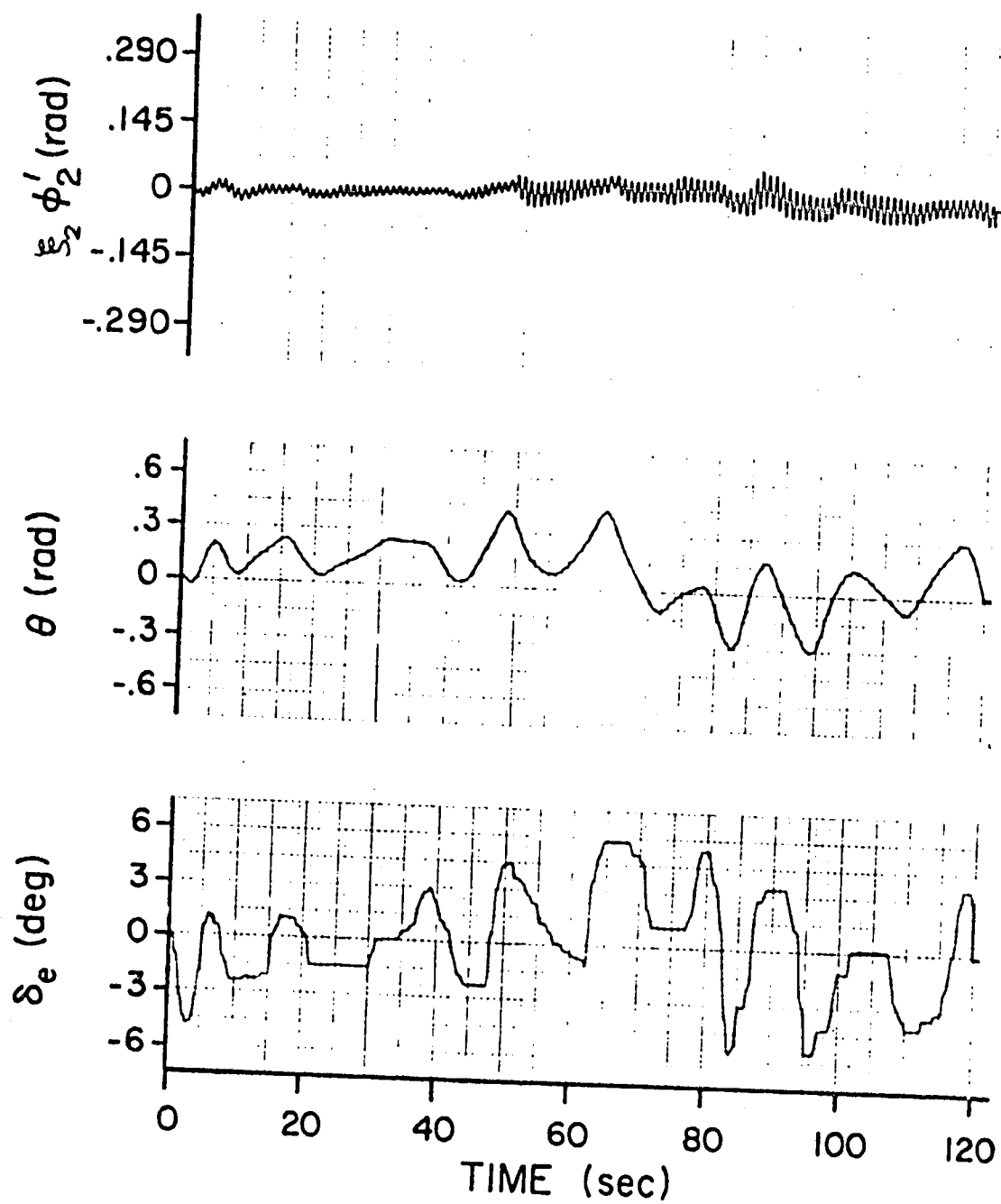
-B-

Figure 4. (Continued)

CHAPTER III

EQUATIONS OF MOTION

The equations of a flexible airplane consist of an overall spatial motion, that is, a rigid body motion, and a local deformation due to its inherent flexibility. The basic principles underlying the equations of motion are the conservation of the linear and angular momenta and an internal equilibrium due to elastic deformation. The equations are written in terms of the x,y,z body-fixed axes frame of reference. The orthogonal axes are chosen such that the x-axis passes through the center of gravity of the airplane and points forward parallel to the free stream steady-state(trim) velocity, the y-axis points out to the right wing, and z-axis points downward.

The deformation of the airplane is expressed in terms of natural mode shapes and generalized coordinates. The airplane is assumed to be a plate like structure in the normal mode (in-vacuum vibration modes) calculation.

In the next four sections the pertinent assumptions and the equations of motion are summarized. The detailed derivation and related discussions can be found in [11-14].

Small Perturbation Equations of Motion

For a cruise, level flight condition at a trim speed U_o, the small perturbation longitudinal equations of motion are given by:

$$m\dot{u} = -mg\theta + X_u(u + u_g) + X_\alpha(\alpha + \alpha_g) + X_{\delta_c}\delta_c$$

$$mU_o(\dot{\alpha} - \dot{\theta}) = Z_u(u + u_g) + Z_\alpha(\alpha + \alpha_g) + Z_{\dot{\alpha}}(\dot{\alpha} - q_g) + Z_{\dot{\theta}}(\dot{\theta} + q_g)$$

$$+ Z_{\delta e}\delta e + \sum_{i=1}^{\infty}[\frac{\partial Z}{\partial \xi_i}\xi_i + \frac{\partial Z}{\partial \dot{\xi}_i}\dot{\xi}_i]$$

$$I_y\ddot{\theta} = M_u(u + u_g) + M_\alpha(\alpha + \alpha_g) + M_{\dot{\alpha}}(\dot{\alpha} - q_g) + M_{\dot{\theta}}(\dot{\theta} + q_g) \qquad (3.1)$$

$$+ M_{\delta e}\delta e + \sum_{i=1}^{\infty}[\frac{\partial M}{\partial \xi_i}\xi_i + \frac{\partial M}{\partial \dot{\xi}_i}\dot{\xi}_i]$$

$$m_i[\ddot{\xi}_i + 2\zeta_i\omega_i\dot{\xi}_i + \omega_i^2\xi_i] = (\frac{\partial Q_{\xi_i}}{\partial \alpha})(\alpha + \alpha_g) + \frac{\partial Q_{\xi_i}}{\partial q}(\dot{\theta} + q_g)$$

$$+ (\frac{\partial Q_{\xi_i}}{\partial \delta_e})\delta_e + (\frac{\partial Q_{\xi_i}}{\partial \dot{\alpha}})(\dot{\alpha} - q_g) + \sum_{k=1}^{\infty}[\frac{\partial Q_{\xi_i}}{\partial \xi_k}\xi_k + \frac{\partial Q_{\xi_i}}{\partial \dot{\xi}_k}\dot{\xi}_k], \quad i=1,2,..$$

where:

$(\dot{\ }) \equiv d(\ )/dt$

u Perturbation forward speed

u_g Perturbation of u due to gust

θ Perturbation pitch angle (rad)

q Perturbation pitch angle rate (rad/s), $(q \equiv \dot{\theta})$

q_g Perturbation of q due to gust

α Perturbation of angle of attack (rad)

α_g Perturbation of α due to gust

δ_e Perturbation of elevator deflection (rad)

ξ_i Generalized coordinate of the ith elastic mode

m_i Generalized mass of the ith elastic mode

Q_{ξ_i} Generalized force of the ith elastic mode

ω_i in-vacuum elastic mode undamped natural frequency of ith mode

The equations (3.1) are rewritten in a state-variable formulation as:

$$\dot{x}_a(t) = A_a x_a(t) + B_a u_a(t) + E_a w_a(t) \tag{3.2}$$

where

$$x_a(t) = \text{col. } [u_g, \alpha_{g_1}, \alpha_g, q_g, u, \alpha, \theta, \dot{\theta}, \xi_1, \xi_2, \ldots, \dot{\xi}_1, \dot{\xi}_2, \ldots]$$

$$u_a(t) = \delta_e$$

The state α_{g_1} and the input vector $w_a(t)$ are to be discussed in the next section on the turbulence model.

Turbulence Model

The turbulence model is derived from the Dryden gust power spectra which have the forms [1].

$$\phi_{u_g}(\omega) = \sigma_u^2 \frac{2L_u}{U_o} \frac{1}{1 + (\frac{L_u}{U_o}\omega)^2}$$

$$\phi_{w_g}(\omega) = \sigma_w^2 \frac{L_w}{U_o} \frac{1 - 3(\frac{L_u}{U_o}\omega)^2}{[1 + (\frac{L_w}{U_o}\omega)^2]^2}$$

$$\phi_{\alpha_g}(\omega) = \frac{1}{U_o^2} \phi_{w_g}(\omega)$$

$$\phi_{q_g}(\omega) = \frac{(\frac{\omega}{U_o})^2}{1 + (\frac{4b_w}{\pi}\frac{\omega}{U_o})^2} \phi_{w_g}(\omega)$$

where

$$\sigma_i^2 = \frac{1}{2\pi} \int_\infty^\infty \phi_i(\omega)\, d\omega, \quad i = u_g, w_g, \alpha_g, \text{ and } q_g$$

ω temporal frequency (rad/s)

U_o true air speed

b_w wing span

L_u, L_w gust scale factors which depend on the altitude

The time domain representation of the turbulence as a shaping filter with zero mean, gaussian, white noise processes n_1, and n_2 as inputs is:

$$
\begin{bmatrix} \dot{u}_g \\ \dot{\alpha}_{g_1} \\ \dot{\alpha}_g \\ \dot{q}_g \end{bmatrix} = [A_g] \begin{bmatrix} u_g \\ \alpha_{g_1} \\ \alpha_g \\ q_g \end{bmatrix} + [G] \begin{bmatrix} n_1 \\ n_2 \end{bmatrix}
$$

where

$$
[A_g] = \begin{bmatrix}
-\dfrac{U_o}{L_u} & 0 & 0 & 0 \\[2ex]
0 & -\dfrac{U_o}{L_w} & 0 & 0 \\[2ex]
0 & -(\sqrt{3}-1)\dfrac{\sigma_w}{L_w}\sqrt{\dfrac{U_o}{L_w}} & -\dfrac{U_o}{L_w} & 0 \\[2ex]
0 & -(\sqrt{3}-1)\dfrac{\pi\sigma_w}{4b_w}\dfrac{U_o}{L_w}\sqrt{\dfrac{U_o}{L_w}} & -\dfrac{\pi U_o^2}{4b_w L_w} & -\dfrac{\pi U_o}{4b}
\end{bmatrix}
$$

$$
[G] = \begin{bmatrix}
\sigma_u\sqrt{\dfrac{2U_o}{L_u}} & 0 \\[2ex]
0 & 1 \\[2ex]
0 & \dfrac{\sigma_w\sqrt{3}}{\sqrt{U_o L_w}} \\[3ex]
0 & \dfrac{\pi\sigma_w\sqrt{3}}{4b_w}\sqrt{\dfrac{U_o}{L_w}}
\end{bmatrix}
$$

and

$$E\left\{\begin{bmatrix} \eta_1 \\ \eta_2 \end{bmatrix} \begin{bmatrix} \eta_1 & \eta_2 \end{bmatrix}\right\} = \begin{bmatrix} 1 & 0 \\ 0 & 1 \end{bmatrix}$$

Attitude Director Equations

The total pitch angle time history that the pilot feels and sees, either on the outside horizontal or the attitude indicator display, is given by [10]:

$$y_a(x_p, t) = \theta(t) - \sum_{i=1}^{n} \phi_j'(x_p) \, \xi_j(t) \tag{3.5}$$

$$= \theta(t) - \theta_e(x_p, t)$$

where x_p indicates pilot fuselage station, $\phi_j'(x_p)$ the slope of the jth symmetric elastic mode at that station, $\theta(t)$ the rigid body pitch angle, and $\theta_e(t)$ the elastic contribution to the total pitch angle (Figure 5).

The equation (3.5) can be written in terms of the state variables defined in equation (3.2) as follows:

$$y_a(t) = C_a x_a(t)$$

where

$$C_a = \text{col.} \ [0,0,0,0,0,0,1,0,-\phi_1',-\phi_2',\ldots,0,0,\ldots]$$

RIGID BODY

FLEXURE BODY

U_0

Θ

HORIZON

Z

TANGENT TO FLEXURE
BODY AT COCKPIT

RIGID BODY

FLEXURE BODY

$\sum\limits_{j=1}^{n} \phi_j'(x_p)\xi_j(t)$

$\Theta(t)$

LOCAL HORIZON

Θ_i

$$\Theta_i = \Theta(t) - \sum_{j=1}^{n} \phi_j'(x_p)\xi_j(t)$$
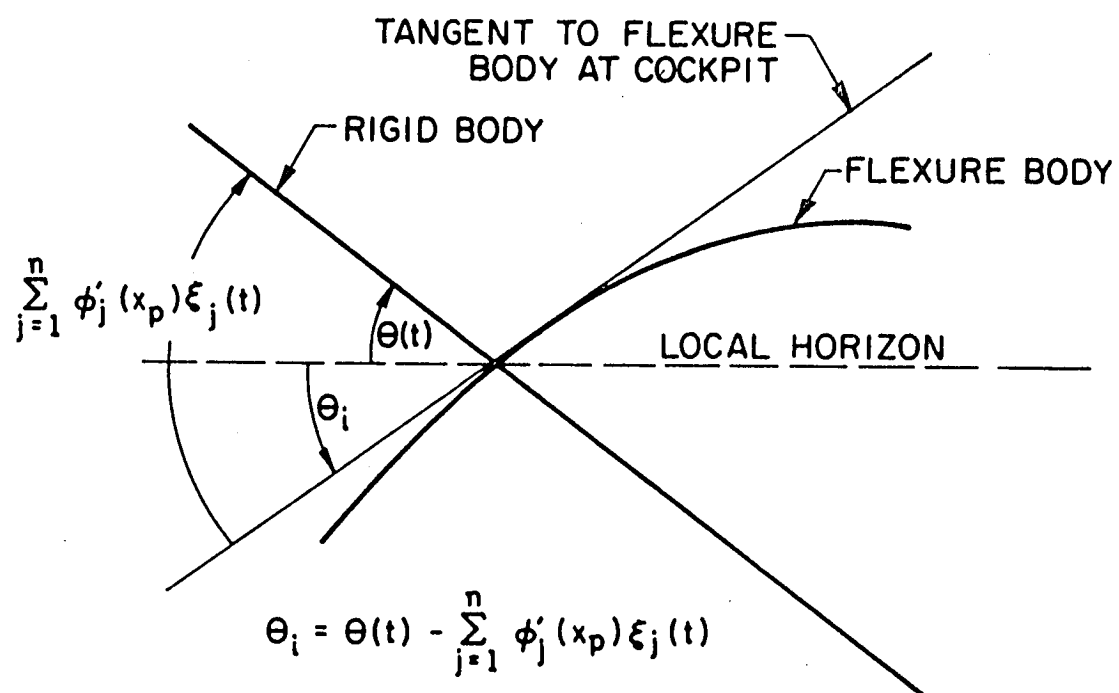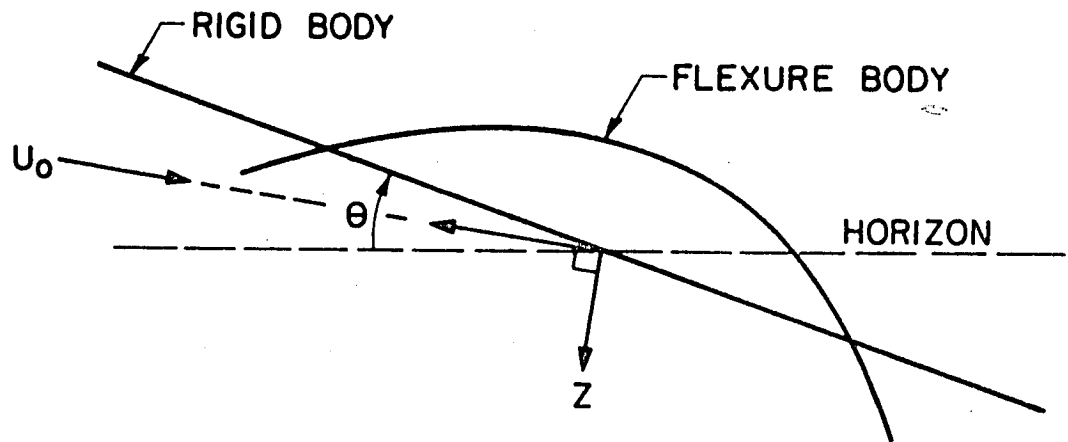
Figure 5. Rigid And Elastic Pitch Angles

B-1 Flight Condition

The B-1 bomber was chosen for this study because it exemplifies the trend toward more elastic structures for future large aircraft. The total length of the B-1 is 46 m (151 ft.). The reference wing span utilized at the flight condition in Table II is 41.7 m (136.67 ft.). The values of the stability derivatives and the necessary data for the equations of motion are given in Appendix A.

TABLE II

B-1 FLIGHT CONDITION

Mass = 103,370.15 kg (7085.0 slugs)

Mach No. = 0.85

Velocity = 289.4 m/s (949.0 fps)

cg at fuselage station = 40.67 m (1061.2 in)

$I_y = 8.0 \times 10^6$ kg-m^2 (5.9 x 10^6 slug - ft^2)

$S_w = 180.8$ m^2 (1946.0 ft^2)

$\bar{c}_w = 4.67$ m (15.33 ft)

$b_w = 41.7$ m (136.67 ft)

CHAPTER IV

PILOT MODELING

The human pilot in a manual control task can be modeled as an active feedback element in the aircraft control system. The quasi-linear model and the optimal control model (OCM) are the two models widely used in this way. The quasi-linear model has the analytical description in terms of the frequency-domain control system design technique, while the optimal control model is based on the time-domain or optimal control theory. Since the analysis in this study is mostly in the time-domain, the optimal control model is employed through out. There are other reasons for employing the optimal control model which will be discussed later.

The optimal control model of the human pilot was originally developed by Kleinman, Baron and Levison [9]. The fundamental assumption underlying the OCM is that the well-motivated, well-trained human pilot will act in a near optimal manner subject to the pilot's internal limitations and understanding of the task. By specifying human limitations, the optimality assumption gives a model that adapts to task specifications and requirements automatically and not through a subsidiary set of adjustment rules as has been done in the quasi-linear model. Thus, for a new situation, the optimal control model can be modified by just determining the operative limitations and the

new control task. The review of the past applications of the model can be found in reference [15].

Model Description

The structure of the optimal control model of human pilot response is shown in Figure 6. The aircraft dynamics, which also include noise shaping filters of the turbulence, are described by the linear, time invariant equations.

$$\dot{x}_a(t) = A_a x_a(t) + B_a u_a(t) + E_a w_a(t) \qquad (4.1)$$

$$x_a(0) = \text{given}$$

where

$x_a(t)$ = aircraft and shaping filters state vector of dimension Na

$u_a(t)$ = pilot's control input vector of dimension Nu

$w_a(t)$ = disturbance vector of dimension Nw, each of which is an independent zero mean, Guassian white noise process with covariance

$$E \{w_{a_i}(t) \ w_{a_i}(\sigma)\} = W_i \delta(t-\sigma), \ i = 1,2,\ldots, Nw \qquad (4.2)$$

The display variables are given by a linear combination of state variables.

$$y_a(t) = C_a x_a(t) \qquad (4.3)$$

where

$y_a(t)$ = displayed vector of dimension Ny
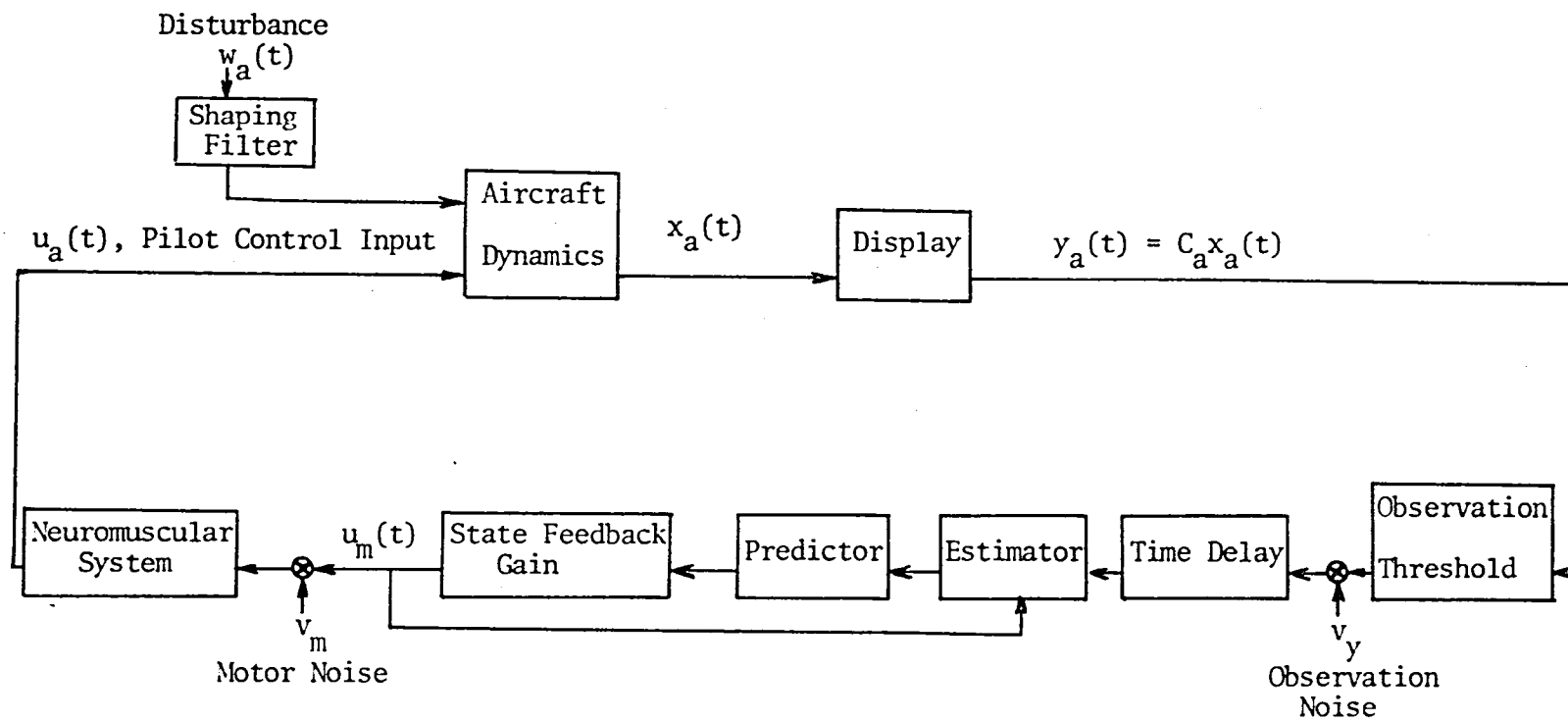
Figure 6. Optimal Control Model of Human Pilot Response

The usual assumption in the model is that if a quantity y_i is explicitly displayed to the pilot, he also derives the rate of change $\dot{y}_i$. Thus, $y_a(t)$ contains both position and velocity information of a displayed signal, but no higher derivative information.

Internal Model

The information processor in the pilot model operates on a noisy, delayed version of the displayed variables to obtain a "best" estimate of the aircraft state vector. This is accomplished by a Kalman filter and a least-mean-square predictor and makes use of an internal model. The internal model of the pilot may be considered to consist of [16].

1. Knowledge about the overall behavior of the aircraft under control and about the possibilities to control it.

2. Knowledge about the disturbances acting on the aircraft and the way they will influence it. This knowledge will be of a statistical nature.

3. Knowledge about the task to be performed.

In many instances, the assumption that the internal model is an exact replica of the system model, i.e., perfect internal model, appears to be a satisfactory one [17]. There are situations in which the assumption of a perfect internal model does not appear tenable. In a highly complex system, i.e., one with a large number of state variables, with a single display it is unlikely to be modeled perfectly by the pilot.

It is of interest in this study to determine the effects of high frequency oscillation, contributed mainly by the elastic modes, on the handling qualities and pilot rating. From a past experiment with ground based simulation of the elastic airplane [8], the pilot action

in a pitch tracking task closely resembles that of the rigid body pitch error rather than the total error displayed to him. This shows the pilot's ability to filter out the high frequency oscillation in the total pitch response and leads to a hypothesis that the pilot uses the slowly varying dynamics subsystem as the internal model.

The decomposition of the slowly varying dynamics from the aircraft/ disturbance dynamics, Eqns. (4.1) and (4.3), is accomplished by the singular perturbation technique (Appendix B). The aircraft/disturbance dynamics can be written in the form:

$$\dot{x}_1(t) = A_{11}x_1(t) + A_{12}x_2(t) + B_1u_a(t) + E_1w_a(t) \tag{4.4}$$

$$\mu\dot{x}_2(t) = A_{21}x_1(t) + A_{22}x_2(t) + B_2u_a(t) + E_2w_a(t)$$

$$y_a(t) = C_1x_1(t) + C_2x_2(t)$$

where

$x_1(t)$ = rigid body and noise shaping filters state vector

$x_2(t)$ = elastic modes state vector

μ = a small positive parameter which arises due to the presence of high frequency elastic modes and can be an unknown in this analysis.

Then, by letting $\mu \to 0^+$ we get

$$\dot{x}_d(t) = A_d\, x_d(t) + B_d u_a(t) + E_d w_d(t)$$
$$y_d(t) = C_d\, x_d(t) + D_d u_a(t) \tag{4.5}$$

where

$$A_d = A_{11} - A_{12}\, A_{22}^{-1}\, A_{21}$$

$$B_d = B_1 - A_{12}\, A_{22}^{-1}\, B_2$$

$$C_d = C_1 - C_2\, A_{22}^{-1}\, A_2$$

$$D_d = D - C_2\, A_{22}^{-1}\, B_2$$

$$E_d = E_1 - A_{12}\, A_{22}^{-1}\, E_2 \qquad \text{This is provided } A_{22}^{-1} \text{ exists.}$$

By using an imperfect internal model, the computational task becomes formidable since it involves the solution of the matrix delay differential equation [17]. The structure of the original optimal control model can be modified from Figure 6 to that of Figure 7. This modification does not affect the prediction capability of the model very much as has been shown in references [17-19]. In this modified model, the pure time delay τ is approximated by a first-order Pade polynomial. Thus, the relation between $u_a(t)$ and $r(t)$ in Figure 7, which was originally expressed by

$$u_a(t) = r(t-\tau) \tag{4.6}$$

or in the Laplace transform operator s,

$$u_a(s) = e^{-\tau s} r(s) \tag{4.7}$$

is now approximated by

$$u_a(s) \approx \frac{-s + 2/\tau}{s + 2/\tau} r(s) \tag{4.8}$$

which can be expressed in the state variable form as

$$u_a(t) = z(t) - r(t) \tag{4.9}$$

where

$$\dot{z}(t) = -\frac{2}{\tau} I \, z(t) + \frac{4}{\tau} I \, r(t) \tag{4.10}$$

I is an identity matrix of appropriate dimension. The time delay τ is normally 0.1 to 0.2 sec.

Human Limitations

Other than the time delay, the pilot has inherent limitations of perceptual noise and perceptual indifference thresholds on displayed information. The time delay has been compensated for in the control action as shown in Eqns. (4.9) and (4.10). The other quantities are associated with the observation process in the pilot model, so the
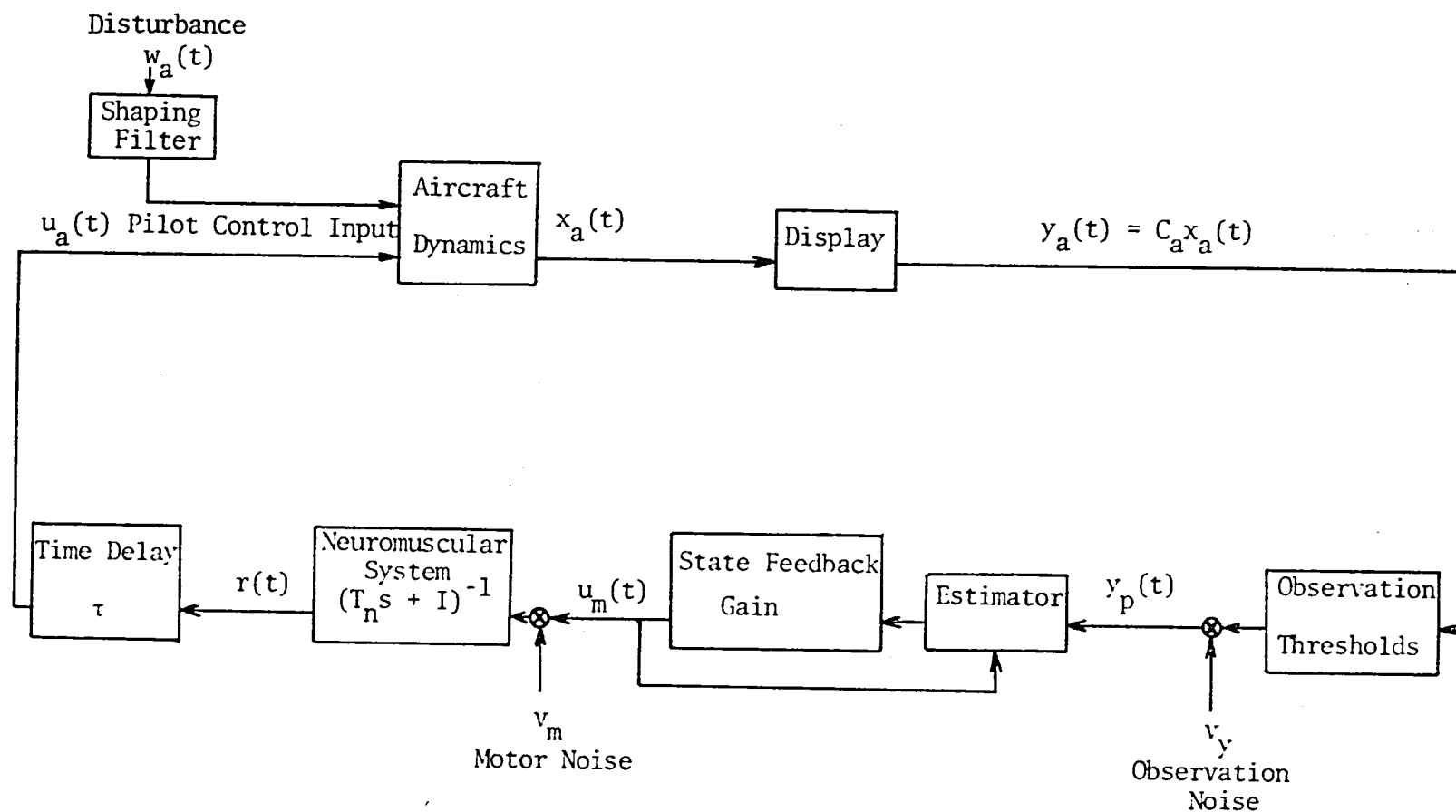
Figure 7. Modified Optimal Control Model of Human Pilot Response

pilot is assumed to perceived $y_p(t)$ which is a noisy version of $y_a(t)$, i.e.,

$$y_p(t) = y_a(t) + v_y(t)$$

(4.11)

where the observation threshold is replaced by the Random Input Describing Function $N(\sigma)$ and incorporated in the observation noise, $v_y(t)$ is a zero-mean, gaussian, white noise process with autocovariance,

$$E\{v_{y_{a_i}}(t) \, v_{y_{a_i}}(\sigma)\} = V_{y_i}(t-\sigma), \quad i=1,2,\ldots, N_y$$

(4.12)

When directly viewing $y_{a_i}(t)$, the associated covariance V_{y_i} is:

$$V_{y_i} = \frac{e^o_{y_i}}{f_i} \hat{\sigma}^2_i$$

(4.13)

where

$$\hat{\sigma}_i = \sigma_{y_i} \, N(\sigma_{y_i})^{-1}$$

$$\sigma_{y_i} = \sqrt{E\{y^2_{a_i}(t)\}}$$

$N(\sigma_{y_i}) = \mathrm{erfc}(\frac{a_i}{\sigma_{y_i}\sqrt{2}})$, describing function gain of threshold

erfc = error function

a_i = half width of dead zone element

$\rho^o_{y_i}$ = noise/signal ratio at full attention on indicator i

= 0.01π or -20 dB normalized power density level

f_i = attention allocation to display indicator i

For the total of k indicators, neglecting the time spent in interinstrument scanning, we have

$$\sum_{i=1}^{k} f_i = 1, \quad 0 < f_i < 1$$

(4.14)

The value of f_i is chosen such that the cost functional of the pilot model is minimized.

Task Definition

The important assumption about the optimal control pilot model is that the pilot's control task is adequately reflected in the choice of a control $r(\cdot)$ that minimizes the cost functional of the form

$$J(r) = \lim_{T \to \infty} E\{ \frac{1}{T} \int_0^T [y_a'(t)Q_y y_a(t) + \dot{r}'(t)Q_R \dot{r}(t)]dt \} \tag{4.15}$$

conditioned on the perceived information $y_p(\cdot)$. Q_y is a specified constant, symmetric, nonnegative definite matrix which depends on the task specification. The control rate term is used to account for the pilot's limitation on the rate of control motion and introduces first-order neuromuscular dynamics in the pilot model.

The selection of the weighting Q_y = diag. $[q_{y_i}]$ is such that

$$q_{y_i} = \left| \frac{1}{y_{pi, max}} \right|^2 \tag{4.16}$$

where

$y_{pi,max}$ is the maximum desired or allowable value of y_{pi}. Unlike Q_y, the weighting Q_R = diag. $[q_{r_i}]$, a positive definite matrix, is not specified before the pilot model equations are solved. It can be shown that the pilot control law which minimizes (4.15) takes the following form:

$$T_n \dot{r}(t) = -r(t) + u_m(t) + v_m(t) \tag{4.17}$$

The matrix T_n is assumed to be in the form T_n = diag. $[t_{n_i}]$, i=1,2,..., Nu. The scalars t_{n_i} are a neuromuscular time constant of human limbs, which has a typical value of 0.1 sec., independent of the system to be controlled. Thus, the weighting q_{r_i} are adjusted iteratively until each $t_{n_i} \approx 0.1$ sec. If the resulting q_{r_i} weighting is such that $1/\sqrt{q_{r_i}}$ is much greater than the physical rate at which one can move

control r_i, then $q_{r_i} = \left| 1/t_i \ (t), \max \right|^2$ must be used. Though, this rarely happens except for highly unstable aircraft dynamics or an aircraft flying through very severe turbulence.

The motor noise $v_m(t)$ is a zero-mean, gaussian, white noise process, with autocovariance

$$E\{v_m(t) \ v_m(\sigma)\} = V_m \delta(t-\sigma) \tag{4.18}$$

and V_m is known to scale with $E\{m_i^2(t)\}$, i.e.,

$$V_{m_i} = \rho_{m_i} \ E\{m_i^2(t)\} \tag{4.19}$$

where the typical value of the motor noise/signal ratio $\rho_{m_i} = 0.003\pi$.

Equations (4.9) and (4.10) may now be augmented to Eqn. (4.1) to define an augmented system of equations

$$\dot{x}_c(t) = A_c x_c(t) + B_c u_m(t) + E_c w_c(t) \tag{4.20}$$

$$y_a(t) = C_c x_c(t)$$

where

$$x_c = [x_a, z, r]'$$

$$A_c = \begin{bmatrix} A_a & B_a & -B_a \\ 0 & -2/\tau & 4/\tau \\ 0 & 0 & -T_n^{-1} \end{bmatrix}$$

$$B_c = [0, \ 0, \ T_n^{-1}]'$$

$$C_c = [C_a, \ 0, \ 0]$$

$$E_c = \begin{bmatrix} E_a & 0 \\ 0 & 0 \\ 0 & T_n^{-1} \end{bmatrix}$$

$$w_c = [w, \ v_m]'$$

Equation (4.20) is the "actual" dynamics to be controlled by the pilot.

The Pilot Model

The pilot's control input $r(t)$ that minimizes $J(r)$ is generated based on the augmented system of the internal model (4.5) and the delay compensation (4.9) and (4.10), i.e.,

$$\dot{x}_s(t) = A_s \, x_s(t) + B_s r(t) + E_s w(t)$$

$$y_s(t) = C_s \, x_s(t) + D_s r(t)$$

(4.21)

where

$$x_s = \begin{bmatrix} x_d \\ z \end{bmatrix}$$

$$A_s = \begin{bmatrix} A_d & B_d \\ 0 & -2/\tau \end{bmatrix}$$

$$B_s = \begin{bmatrix} -B_d \\ 4/\tau \end{bmatrix}$$

$$C_s = [C_d, \, D_d]$$

$$D_s = [-D_d]$$

$$E_s = \begin{bmatrix} E_d \\ 0 \end{bmatrix}$$

The command control of the pilot is given by

$$u_m(t) = -L_{opt} \, x_s(t)$$

$$= -L^* x_t(t)$$

(4.22)

where

$$L^* = [L_{opt} \, 0]$$

$$x_t = \begin{bmatrix} x_s \\ r \end{bmatrix}$$

$$L_{opt} = P_{22}^{-1} \, Q_R$$

$$T_n = P_{22}^{-1} P_{12}$$

$$P = \begin{bmatrix} P_{11} & P_{12} \\ P_{12} & P_{22} \end{bmatrix}$$

satisfies the equation

$$A_o' P + PA_o + C_o' Q_y C_o - PB_o Q_R^{-1} B_o' P = 0 \tag{4.23}$$

where

$$A_o = \begin{bmatrix} A_s & B_s \\ 0 & 0 \end{bmatrix}$$

$$B_o = \begin{bmatrix} 0 \\ I \end{bmatrix}$$

$$C_o = [C_s \quad D_s]$$

The state $x_t(t)$ is the best estimate of $x_t(t)$ generated by a Kalman filter

$$\dot{\hat{x}}_t(t) = A_t \hat{x}_t(t) + B_t u_m(t) + K[y_p - C_o \hat{x}_t(t)] \tag{4.24}$$

where

$$K = \Sigma C_o' V_y^{-1} \tag{4.25}$$

and Σ satisfies the equation

$$A_t \Sigma + \Sigma A_t' + E_o W_t E_o' + \Sigma C_o' V_y^{-1} C_o \Sigma = 0 \tag{4.26}$$

where

$$A_t = \begin{bmatrix} A_s & B_s \\ 0 & -T_n^{-1} \end{bmatrix}$$

$$B_t = \begin{bmatrix} 0 \\ T_n^{-1} \end{bmatrix}$$

$$E_o = \begin{bmatrix} E_s & 0 \\ 0 & T_n^{-1} \end{bmatrix}$$

$$W_t = \begin{bmatrix} W & 0 \\ 0 & V_m \end{bmatrix}$$

Combining equations (4.11) with (4.20), (4.22) and (4.24) yields the closed loop system

$$\dot{x}_c(t) = A_c x_c(t) - B_c L \hat{x}_t(t) + E_c w_c(t)$$

$$\dot{\hat{x}}_t(t) = (A_1 - B_1 L)\hat{x}_t + K[C_c x_c - C_o \hat{x}_t + v_y(t)]$$

(4.27)

or

$$\dot{\psi} = F\psi + Gw$$

(4.28)

where

$$\psi = \begin{bmatrix} x_c \\ x_t \end{bmatrix}$$

$$F = \begin{bmatrix} A_c & -B_c L^* \\ KC_c & A_1 & -B_1 L^* & -KC_o \end{bmatrix}$$

$$G = \begin{bmatrix} E_c & 0 \\ 0 & K \end{bmatrix}$$

$$w = \begin{bmatrix} w_c \\ v_y \end{bmatrix}$$

Thus,

$$\text{cov } \psi = \begin{bmatrix} \text{cov } x_c x_c' & \text{cov } x_c x_t' \\ \text{cov } x_t x_c' & \text{cov } x_t x_t' \end{bmatrix} \equiv \Psi$$

(4.29)

is the solution of

$$\dot{\Psi} = F\Psi + \Psi F' + G\Omega G'$$

(4.30)

where

$$\Omega = \begin{bmatrix} W_c & 0 \\ 0 & V_y \end{bmatrix}$$

Pilot Opinion Rating Technique

Hess [18] has formulated a pilot rating technique for the optimal control pilot modeling procedure. The technique has been successfully validated in a variety of tasks [18, 20]. The rating technique can be stated as follows:

If

(1) the index of performance and model parameters in the optimal control pilot modeling procedure yield a dynamically representative model of the human pilot,

(2) the variables selected for inclusion in the index of performance are directly observable by the pilot,

(3) the weighting coefficients in the index of performance are chosen as the squares of the reciprocals of maximum "allowable" deviations of the respective variables, and these deviations are consonent with the task as perceived by the pilot.

Then

the numerical value of the index of performance resulting from the modeling procedure can be related to the numerical pilot rating which the pilot assigns to the vehicle and task by

$$P.O.R. = 2.51 \ln (10 \ J) + 0.3$$

where   (4.31)

P.O.R. = pilot opinion rating on Cooper-Harper scale

J   = value of the performance index

Computational Algorithms

There are two major computer programs developed in this work for predictions of pilot rating and standard deviations of the response variables

for a piloted-aircraft manual control task. A digital computer program
STDOCM is a modification and extension of the program PIREP [21] written
for operation on CDC-6600 at Wright Patterson Air Force Base to implement
the standard optimal control model of the human pilot. A program MODOCM
is developed to implement the modified optimal control model of the human
pilot which is presented in this chapter. Both programs are written in
Fortran IV for operation on IBM system 370/168 at Oklahoma State Univer-
sity and are available from Professor R. L. Swaim, School of Mechanical
and Aerospace Engineering, Oklahoma State Unversity.

CHAPTER V

EFFECTS OF ELASTIC MODES INTERACTION
ON HANDLING QUALITIES

The elastic modes interaction with the rigid body dynamics is intro-
duced to the large flexible aircraft model by parametric lowering of the
undamped natural frequencies of the two elastic modes. This will cause
controlling the rigid pitch angle by observing the total pitch error to
become more difficult as indicated in the past experimental results [8].
The standard optimal control model for the human pilot and modified model
presented in Chapter IV are applied to the illustrated cases of varying
elastic modes interaction. It will be shown that the standard optimal
control model gives the misleading results when there is a severe modes
interaction between the elastic modes and the rigid body dynamics. The
modified model gives more consistent results with the experimental data
on the effects of elastic modes and the rigid body dynamics. The modified
model gives more consistent results with the experimental data on the ef-
fects of elastic modes interaction on handling qualities and pilot ratings
than that of the standard optimal control model. In this chapter the il-
lustrated cases used in the computer simulation study are described. Then
the simulation results are presented. Finally, the separation boundary
which can be used as an indicator of when the pilot can or cannot visually
separate the rigid body motion from the total motion is presented.

The Illustrated Cases

The ten illustrated cases are obtained from the equations of motion (3.1) in which the natural frequencies of the two elastic modes are parametrically reduced. Dynamic characteristics of each case are specified by four modes: phugoid mode, short period mode, elastic mode 1, and elastic mode 2 as shown in Table III. These ten cases will exemplify most of the situations in which the handling qualities and pilot ratings would be affected differently by the two elastic modes included in the model.

The lowering of the elastic mode natural frequencies resulted in mode interaction which lowered the coupled short-period and phugoid frequencies or made one of them split into positive and negative real roots. A full state feedback control law is used to place the roots of the characteristic equation at precise values for each case. The rigid body dynamics are maintained to be the same as Case 1 and the elastic mode coupled frequencies placed at original values before the state feedback control law was applied. This will ensure that the pilot ratings are based on the relative amplitudes of rigid and elastic pitch angle responses and not on poor rigid body dynamics.

The simulation results on the ten cases by using the standard optimal control model (OCM) for the human pilot and the modified model are shown in Tables IV and V, respectively. These results clearly indicate that when there are severe modes interaction, such as Cases #3, 6 and 9, the standard OCM gave very low pilot ratings predictions which are inconsistent with the experimental results [8]. In contrast the modified OCM gave more consistent results since it includes the visual separation process of the rigid body response from the elastic modes response which the pilot has to accomplish when the amplitude of the high frequency

TABLE III

NATURAL FREQUENCIES AND DAMPING RATIOS OF TEN CASES

Case #	ω_1 rad/s	ω_2 rad/s	ω_{ph} rad/s	ζ_{ph}	ω_{sp} rad/s	ζ_{sp}	ω_{1e} rad/s	ζ_{1e}	ω_{1e} rad/s	ζ_{2e}
1	13.59	21.18	.0665	.0312	2.9334	.5209	13.236	.0497	21.395	.02112
2	8	21.18	.04614	.001376	2.581	.4992	7.508	.1127	21.390	.02104
3	4	21.18	.1412	.1336	Real Roots + 1.652 - 2.266		4.544	.3892	21.380	.02102
4	13.59	15.00	.06345	.02899	2.889	.5247	13.04	.04508	15.480	.03052
5	8	15.00	.04489	.001946	2.586	.5031	7.400	.1073	15.340	.02787
6	4	15.00	.1411	.134	Real Roots + 1.568 - 2.172		4.356	.3990	15.320	.02761
7	13.59	13.59	.06203	.02797	2.87	.5262	12.76	.03821	14.380	.02923
8	8	13.59	.04433	.002208	2.588	.5048	7.345	.1042	13.990	.03117
9	4	13.59	.1411	.1350	Real Roots + 1.527 - 2.126		4.269	.4035	13.970	.03062
10	8	8	.03801	.005574	2.608	.5245	6.403	.04999	9.390	.08138

TABLE IV

PERFORMANCE PREDICTION BY THE STANDARD OCM

CASE #	θ_{rms} (deg)	$\dot{\theta}_{rms}$ (deg/s)	δ_{rms} (rad x 10^3)	P. O. R.
1	.3895	1.650	1.143	1.0
2	.5422	2.343	2.475	2.6
3	.5042	1.573	2.234	1.0
4	.3612	0.917	0.910	1.0
5	.5096	2.335	2.266	2.5
6	.4604	1.721	2.061	1.2
7	.3437	1.127	1.392	1.0
8	.4955	2.288	2.142	2.4
9	.4445	1.750	2.000	1.2
10	.3833	1.591	2.810	1.0

TABLE V

PERFORMANCE PREDICTION BY THE MODIFIED OCM

CASE #	θ_{rms} (deg)	$\dot{\theta}_{rms}$ (deg/s)	δ_{rms} (rad x 10^3)	P.O.R.
1	.3663	1.848	0.829	1.2
2	.5724	2.832	1.199	3.3
3	.8123	3.721	1.014	4.7
4	.3157	0.999	1.024	1.0
5	.5345	2.746	1.195	3.2
6	.7374	3.470	0.872	4.3
7	.3228	1.428	0.869	1.0
8	.5172	2.657	1.181	3.0
9	.7043	3.360	0.833	4.1
10	.4187	2.091	1.167	1.8

elastic modes is getting larger. On the other hand, when the modes inter-
action are small, both pilot modeling techniques gave almost the same pre-
dictions.

The Separation Boundary

The separation boundary is defined as the limit of when the pilot can
or cannot visually separate the rigid body motion from the total motion.
The visual separation is essential in controlling the rigid pitch angle or
other rigid body parameter of the elastic airplane when only the total
pitch angle response or a corresponding parameter is available to the pilot.

From Chapter IV, two kinds of pilot modeling techniques are discussed.
The standard OCM is the pilot model that asssumed that the pilot has the
perfect internal model of the aircraft/disturbance dynamics. This model
will give the best possible pilot opinion rating (P.O.R.) in any tracking
task. The other model, the modified OCM, is the one with a slowly varying
internal model. In this model, the pilot is assumed to be able to com-
pletely separate the slowly varying or the rigid body motion from the to-
tal motion. The difference between the P.O.R.'s, i.e., ΔP.O.R., of 2 is
chosen to be a separation boundary. That is if ΔP.O.R. is greater than
or equal to 2, the pilot cannot visually separate the rigid body motion
from the elastic motion in the display.

It is known that the pilot opinion rating depends on many factors
such as the intensity of turbulence and the level of difficulty of the
task. To study the modes interaction effect all other effects should
be kept at their nominal values. That is without severe modes interaction
effect the other parameters should be set such that P.O.R. is equal to 1.
Once the P.O.R. has been initialized for some specific task, the separation

boundary can be found from the P.O.R. prediction of the modified OCM alone. This is because the standard OCM will give almost unity P.O.R. in the severe modes interaction cases, if the rigid body dynamics have been maintained at the known good handling qualities specifications. So, instead of using ΔP.O.R. = 2 as the separation boundary, the modified OCM's P.O.R. of 3 can be equally well used as the separation boundary provided the proper initialization mentioned above has been done.

CHAPTER VI

CONCLUSIONS AND RECOMMENDATIONS

A model for the human pilot in a manual control task using the optimal control techniques has been developed for predicting the handling qualities or the pilot ratings of a large flexible aircraft where the elastic modes interaction with the rigid body dynamics is significant. The separation boundary concept, which will tell when the pilot can or cannot visually separate the rigid body motion from the elastic one, has been introduced. The techniques developed here make it easier to investigate the modes interaction effect on the handling qualities in a preliminary design stage before the first prototype has been built. If the handling qualities are severely affected by the elastic modes interaction with the rigid body dynamics, the elastic modes suppression control system should be designed and implemented along with the stability augmentation system of the rigid body dynamics.

A comparison of the model predictions with the past experimental data shows that the modified optimal control model for the human pilot developed here is much better in predicting the elastic modes effect on the handling qualities than the standard optimal control model. This is due to the fact that the mode decomposition mechanism has been incorporated into the modified model.

However, only one longitudinal trim flight condition was investigated, its validity for different flight conditions can only be confirmed by conducting more investigations.

Future work should also include the computational aspect of the model. In the pilot model parameters identification, it is required to solve an $(n_a + n_s + 4) \times (n_a + n_s + 4)$ matrix equation (4.30) for the modified model instead of solving an $(n_a + 1) \times (n_a + 1)$ matrix equation in the standard OCM, where n_a, dimension of an aircraft/disturbance dynamics, is 12; n_s, dimension of a slowly varying part of the aircraft/disturbance dynamics, is 8. This will risk the numerical instability when one has to include more elastic modes in the aircraft/disturbance dynamics. An alternative structure of the pilot model should be explored to ease the computational burden of the high order aircraft/disturbance system.

SELECTED BIBLIOGRAPHY

(1) Chalk, C.R. et al. Background Information and User Guide for Mil-F-8785B (ASG), Military Specification-Flying Qualities of Piloted Airplanes. AFFDL-TR-69-72, Air Force Flight Dynamics Laboratory, Wright-Patterson AFB, Ohio, 1969.

(2) Lyon, H. M. A Method for Estimation the Effect of Aeroelastic Distortion of a Sweptback Wing on Stability and Control Derivatives. Aeronautical Research Council, Report and Memoranda No. 2331, London, 1946.

(3) McCarthy, J.F., and Kirsch, A.A. Effect of Structural Flexibility on Aircraft Loading. WADC TR 6385, Wright Air Development Center, Wright-Patterson AFB, Ohio, 1953.

(4) Milne, R.D. Dynamics of Deformable Airplane. Aeronautical Research Council Report and Memoranda No. 3345, London, 1964.

(5) Howard, V.W. The Effects of Structural Elasticity on Aircraft Control Systems. WADC TR 56-166, Wright Air Development Center, Wright-Patterson AFB, Ohio, 1956.

(6) Dornfeld, G.M. et al. A Method for Predicting the Stability Characteristics of an Elastic Airplane, Vol. 1, 2, 3, Flexstab 3.01.00 AFFDL-TR-77-55, Air Force Flight Dynamics Laboratory Wright-Patterson AFB, Ohio, 1977.

(7) Roskam, J. Flight Dynamics of Rigid and Elastic Airplanes. Roskam Aviation and Engineering Corporation, Lawrence, Kansas, 1979.

(8) Yen, W.Y. "Effects of Dynamic Aeroelasticity on Handling Qualities and Pilot Rating." (Unpublished Ph.D. Thesis, Purdue University, 1977.)

(9) Kleinman, D.L., Baron, S., and Levison, W.H. "Acontrol Theoretic Approach to Manned Vehicle Systems Analysis." IEEE Trans. on Automatic Control, Vol, AC-16, No. 6 (Dec., 1971), pp. 824-832.

(10) Crother, C.A., Gabelman, B., and Langton D. Structural Mode Effects on Flying Qualities in Turbulence. AFFDL-TR-73-88, Air Force Flight Dynamics Laboratory, Wright-Patterson AFB, Ohio, 1973.

(11) Wykes, J.H. B-1 Flexible Vehicle Equations of Motion for Ride Quality, Terrain Following, and Handling Qualities Studies. Internal Document TFD-71-430-1, North American Rockwell, Los Angeles, CA, 1973.

(12) Roberts, P.A. "Effects of Control Laws and Relaxed Static Stability on Vertical Ride Quality of Flexible Aircraft." (Unpublished Ph.D. Thesis, Purdue University, 1976.)

(13) Taylor, A.S., and Woodcock, D.L. The Dynamics of Deformable Aircraft. Aeronautical Research Council, Report and Memoranda No. 3776, London, 1976.

(14) Swaim, R.L., and Fullman, D.G. "Prediction of Elastic Airplane Longitudinal Dynamics from Rigid-body Aerodynamics." Journal of Aircraft, Vol. 14, No. 9 (1977), pp. 868-873.

(15) Baron, S. "A Brief Overview of the Theory and Application of the Optimal Control Model of the Human Operator." Edited by M.C. Waller: Models of Human Operators in Vision Dependent Tasks. NASA Conference Publication 2103, 1979.

(16) Velduyzen, W., and Stassen, H.G. "The Internal Model Concept: An Application to Modeling Human Control of Large Ships." Human Factors, Vol, 19, No. 4 (1977), pp. 367-380.

(17) Baron, S., and Berliner, J. MANMOD 1975: Human Internal Models and Scene-Perception Models. Army Missile Research, Development and Engineering, Redstone Arsenal, Alabama, 1975.

(18) Hess, R.A. "Prediction of Pilot Ratings Using an Optimal Pilot Model." Human Factors, Vol. 19, No. 5 (1977), pp. 459-475.

(19) Stengel, R.F., Taylor, J.H., Broussard, J.R., and Berry, P.W. High Angle of Attack Stability and Control. ONE-CR215-273-1, The Office of Naval Research, 1976.

(20) Schmidt, D.K. Unified Synthesis of Manual and Automatic Control Applied to Integrated Fire and Flight Control. AFFDL-TM-78-105-FGC, Wright-Patterson Air Force Base, Ohio, 1978.

(21) Curry, R.E., Hoffman, W.C., and Young, L.R. Pilot Modeling for Manned Simulation. AFFDL-TR-76-124, Air Force Flight Dynamics Laboratory, Wright-Patterson AFB, Ohio, 1976.

(22) Chow, J.H., Allemong, J.J., and Kokotovic, P.V. "Singular Perturbation Analysis of Systmes with Sustained High Frequency Oscillation." Automatica, Vol. 14 (1978), pp. 271-279.

(23) Haddad, A.H. "Linear Filtering of Singlarly Perturbed Systems." IEEE Trans, Automat. Control, Vol. AC-21 (1976), pp. 515-519.

(24) Chow, J.H., and Kokotovic, P.V. "A Decomposition of Near-Optimum Regulators for Systems with Slow and Fast Modes." IEEE Trans, Automat. Control, Vol. AC-21 (1976), pp. 701-705.

APPENDIX A

NUMERICAL VALUES OF STABILITY DERIVATIVES

AND EQUATIONS OF MOTION

The low level penetration flight condition for the B-1 was supplied by the B-1 System Program Office at Wright-Patterson AFB from Rockwell International unclassified documents. The stability derivatives used in euqations (3.1) were based on preliminary aerodynamic analyses, but closely representative of the vehicle that has been flying. The relations between dimensional force and moment and elastic force derivatives as a function of nondimensional stability derivatives are given in Table VI and VII, respectively. The non-dimensional stability derivative values for the unqugmented vehicle are given in Table VIII. The gust specifications for the study vehicle are given in Table IX. Finally, the A_{11}, A_{12}, A_{21}/μ, A_{22}/μ, B_1, B_2/μ, C_1, C_2 and E_1 matrices for the unaugmented airplane are given in Tables X to XVIII, respectively. The matrices E_2 and D are zero matrices and the matrices A_a, B_a, C_a and E_a are defined as follows:

$$A_a \equiv \begin{bmatrix} A_{11} & A_{12} \\ A_{21}/\mu & A_{22}/\mu \end{bmatrix}$$

$$B_a \equiv \begin{bmatrix} B_1 \\ B_2/\mu \end{bmatrix}$$

$$C_a \equiv \begin{bmatrix} C_1 & C_2 \end{bmatrix}$$

47

$$E_a \equiv \begin{bmatrix} F_1 \\ F_2/\mu \end{bmatrix}$$

TABLE VI

DIMENSIONAL FORCE AND MOMENT DERIVATIVES AS A FUNCTION OF NON-DIMENSIONAL STABILITY DERIVATIVES

$a_1 = \rho U_o^2 S/2$		$a_2 = a_1 c/2U_o$
$X_u = a_1 C_{x_u}/U_o$	$Z_u = a_1 C_{z_u}/U_o$	$M_u = a_1 c C_{m_u}/U_o$
$X_\alpha = a_1 C_{x_\alpha}$	$Z_\alpha = a_1 C_{z_\alpha}$	$M_\alpha = a_1 c C_{m_\alpha}$
$X_{\dot\alpha} = a_2 C_{x_{\dot\alpha}}$	$Z_{\dot\alpha} = a_2 C_{z_{\dot\alpha}}$	$M_{\dot\alpha} = a_2 c C_{m_{\dot\alpha}}$
$X_\theta = a_2 C_{x_{\dot\theta}}$	$Z_\theta = a_2 C_{z_{\dot\theta}}$	$M_{\dot\theta} = a_2 c C_{m_{\dot\theta}}$
$X_{\delta_e} = a_1 C_{x_{\delta e}}$	$Z_{\delta_e} = a_1 C_{z_{\delta_e}}$	$M_{\delta_e} = a_1 c C_{m_{\delta e}}$
$X_{\delta_e} = 1$	$Z_{\delta_e} = a_1 C_{z_{\delta_e}}$	$M_{\delta_e} = a_1 c C_{m_{\delta e}}$
$X_{\delta_t} = 1$	$Z_{\delta_t} = 0$	$M_{\delta_t} = 0$
$X_{\xi_1} = a_1 C_{x_{\xi_1}}$	$Z_{\xi_1} = a_1 C_{z_{\xi_1}}$	$M_{\xi_1} = a_1 c C_{m_{\xi_1}}$
$X_{\dot\xi_1} = a_1 C_{x_{\dot\xi_1}}/U_o$	$Z_{\dot\xi_1} = a_1 C_{z_{\dot\xi_1}}/U_o$	$M_{\dot\xi_1} = a_1 c C_{m_{\dot\xi_1}}/U_o$
$X_{\xi_2} = a_1 C_{x_{\xi_2}}$	$Z_{\xi_2} = a_1 C_{z_{\xi_2}}$	$M_{\xi_2} = a_1 c C_{m_{\xi_2}}$
$X_{\dot\xi_2} = a_1 C_{x_{\dot\xi_2}}/U_o$	$Z_{\dot\xi_2} = a_1 C_{z_{\dot\xi_2}}/U_o$	$M_{\dot\xi_2} = a_1 c C_{m_{\dot\xi_2}}/U_o$

TABLE VII

DIMENSIONAL ELASTIC FORCE DERIVATIVES AS A FUNCTION OF NON-DIMENSIONAL STABILITY DERIVATIVES

$$a_1 = \rho U_o^2 S/2 \qquad\qquad a_2 = a_1 c/2\, U_o$$

$$Q_{\xi_{1_\alpha}} = a_1 C_{\xi_{1_\alpha}} \qquad\qquad Q_{\xi_{2_\alpha}} = a_1 C_{\xi_{2_\alpha}}$$

$$Q_{\xi_{1_{\dot\alpha}}} = a_2 C_{\xi_{1_{\dot\alpha}}} \qquad\qquad Q_{\xi_{2_{\dot\alpha}}} = a_2 C_{\xi_{2_{\dot\alpha}}}$$

$$Q_{\xi_{1_{\dot\theta}}} = a_2 C_{\xi_{1_{\dot\theta}}} \qquad\qquad Q_{\xi_{2_{\dot\theta}}} = a_2 C_{\xi_{2_{\dot\theta}}}$$

$$Q_{\xi_{1_{\xi_1}}} = a_1 C_{\xi_{1_{\xi_1}}} \qquad\qquad Q_{\xi_{2_{\xi_1}}} = a_1 C_{\xi_{2_{\xi_1}}}$$

$$Q_{\xi_{1_{\dot\xi_2}}} = a_1 C_{\xi_{1_{\dot\xi_2}}}/U_o \qquad\qquad Q_{\xi_{2_{\dot\xi_2}}} = a_1 C_{\xi_{2_{\dot\xi_2}}}/U_o$$

$$Q_{\xi_{1_{\xi_2}}} = a_1 C_{\xi_{1_{\xi_2}}} \qquad\qquad Q_{\xi_{2_{\xi_2}}} = a_1 C_{\xi_{2_{\xi_2}}}$$

$$Q_{\xi_{1_{\dot\xi_2}}} = a_1 C_{\xi_{1_{\dot\xi_2}}}/U_o \qquad\qquad Q_{\xi_{2_{\dot\xi_2}}} = a_1 C_{\xi_{2_{\dot\xi_2}}}/U_o$$

$$Q_{\xi_{1_{\delta_e}}} = a_1 C_{\xi_{1_{\delta_e}}} \qquad\qquad Q_{\xi_{2_{\delta_e}}} = a_1 C_{\xi_{2_{\delta_e}}}$$

TABLE VIII

STABILITY DERIVATIVES FOR B-1 BOMBER
IN MACH 0.85 FLIGHT CONDITION

$C_{x_u} = -0.08066$ $\qquad$ $C_{z_u} = -1.9659$ $\qquad$ $C_{m_u} = -0.4546$

$C_{x_\alpha} = -0.08500$ $\qquad$ $C_{z_\alpha} = -3.9367$ $\qquad$ $C_{m_\alpha} = -1.41052$

$C_{x_{\dot\alpha}} = 0$ $\qquad$ $C_{z_{\dot\alpha}} = -5.0$ $\qquad$ $C_{m_{\dot\alpha}} = -11.005$

$C_{x_{\dot\theta}} = 0$ $\qquad$ $C_{z_{\dot\theta}} = 17.8558$ $\qquad$ $C_{m_{\dot\theta}} = -35.7556$

$C_{x_{\delta_e}} = 0$ $\qquad$ $C_{z_{\delta_e}} = -0.9426$ $\qquad$ $C_{m_{\delta_e}} = -2.799$

$C_{x_{\xi_1}} = 0$ $\qquad$ $C_{z_{\xi_1}} = -0.02922$ $\qquad$ $C_{m_{\xi_1}} = -0.0348$

$C_{x_{\dot\xi_1}} = 0$ $\qquad$ $C_{z_{\dot\xi_1}} = -0.6592$ $\qquad$ $C_{m_{\dot\xi_1}} = -1.32169$

$C_{x_{\xi_2}} = 0$ $\qquad$ $C_{z_{\xi_2}} = 0.015$ $\qquad$ $C_{m_{\xi_2}} = 0.03787$

$C_{x_{\dot\xi_2}} = 0$ $\qquad$ $C_{z_{\dot\xi_2}} = 0.4733$ $\qquad$ $C_{m_{\dot\xi_2}} = 1.233$

$C_{\xi_{1_\alpha}} = -0.06478$ $\qquad$ $C_{\xi_{1_\alpha}} = 0.48975$

$C_{\xi_{1_{\dot\alpha}}} = 0.02469$ $\qquad$ $C_{\xi_{1_{\dot\alpha}}} = 0.48779$

$C_{\xi_{1_{\dot\theta}}} = -1.47658$ $\qquad$ $C_{\xi_{2_{\dot\theta}}} = 3.97547$

$C_{\xi_{1_{\xi_1}}} = 0.00064$ $\qquad$ $C_{\xi_{2_{\xi_1}}} = 0.00451$

TABLE VIII (Continued)

$C_{\xi_1 \dot{\xi}_1} = -0.07243$	$C_{\xi_2 \dot{\xi}_1} = -0.07333$
$C_{\xi_1 \xi_2} = -0.0014$	$C_{\xi_2 \xi_2} = -0.0051$
$C_{\xi_1 \dot{\xi}_2} = 0.0765$	$C_{\xi_2 \dot{\xi}_2} = -0.2588$
$C_{\xi_1 \delta_e} = -0.19635$	$C_{\xi_2 \delta_e} = 0.3939$

TABLE IX

GUST SPECIFICATIONS

Parameters	Value
σ_w	6 fps
σ_u	10.8 fps
L_w	300 ft
L_u	970 ft
U_0	979 fps
b_w	136.68 ft

TABLE X

A_{11} MATRIX

-.9777	0	0	0	0	0	0	0
0	-3.1633	0	0	0	0	0	0
0	-.02604	-3.1633	0	0	0	0	0
0	-.142	-17.25028	-5.4532	0	0	0	0
-.025	0	-25.0000	0	-.025	-25.0	-32.2	0
-6.3408×10^{-4}	0	-1.205	5.6506×10^{-2}	$-.63408 \times 10^{-4}$	-1.205	0	1.03178
0	0	0	0	0	0	0	1.0
-2.292×10^{-3}	0	-7.0672	-1.1112	-2.292×10^{-3}	-7.0672	0	-2.06314

TABLE XI

A_{12} MATRIX

0	0	0	0
0	0	0	0
0	0	0	0
0	0	0	0
0	0	0	0
-8.944×10^{-3}	4.591×10^{-3}	-2.1262×10^{-4}	1.5266×10^{-4}
0	0	0	0
$-.1844$	$.20762$	-70449×10^{-3}	6.9711×10^{-3}

TABLE XII

$A_{21/\mu}$ MATRIX

0	0	0	0	0	0	0	0
0	0	0	0	0	0	0	0
-1.4343×10^{-3}	0	-737.04	-137.51	-1.4353×10^{-3}	-738.04	0	-133.038
-3.9012×10^{-3}	0	752.39	44.3375	-3.9017×10^{-3}	757.39	0	56.4903

TABLE XIII

$A_{22/\mu}$ MATRIX

0	0	1.0	0
0	0	0	1.0
-177.444	61.8964	-1.139	.91536
6.98597	-456.528	-.121926	-.849

TABLE XIV

B_1 MATRIX

0	0	0	0	0	-.28852	0	-15.465

TABLE XV

$B_{2/\mu}$ MATRIX

0	0	-2229.4	613.343

TABLE XVI

C_1 MATRIX

0	0	0	0	0	0	57.2958	0
0	0	0	0	0	0	0	57.2958

TABLE XVII

C_2 MATRIX

-1.4324	-1.66158	0	0
0	0	-1.4324	-1.66158

TABLE XVIII

E_1' MATRIX

5.088	0	0	0	0	0	0	0
0	1	.01948	.10621	0	0	0	0

APPENDIX B

DERIVATIONS RELATED TO SINGULAR PERTURBATION

Consider a singularly perturbed linear time-invariant system

$$\dot{x}_1 = A_{11}x_1 + A_{12}x_2 + B_1 u + E_1 w, \quad x_1(o) = x_{10} \tag{A.1a}$$

$$\mu \dot{x}_2 = A_{21}x_1 + A_{22}x_2 + B_2 u + E_2 w, \quad x_2(o) = x_{20} \tag{A.1b}$$

$$y = C_1 x_1 + C_2 x_2 + v \tag{A.1c}$$

where x_1, x_2, and y are n_1, n_2 and m dimensional vectors respectively, the control u is an r vector, and $\mu > 0$ is a small scalar parameter which arises due to the presence of high frequency elastic modes. The covariances of the p and q dimensional white noise vectors w and v are

$$E\{w(t)\, w'(\tau)\} = W\delta(t-\tau)$$

$$E\{w(t)\, v'(\tau)\} = 0$$

$$E\{v(t)\, v'(\tau)\} = V\delta(t-\tau)$$

Given the observation $y(\tau)$ for $0 < \tau < \infty$, it is desired to estimate $x_1(t)$ which is a slowly varying dynamics vector of the system (A.1).

The conditions that guarantee that high frequency oscillations will occur are n_2 is even and A_{22} has the form [22]

$$A_{22} = \begin{bmatrix} \mu D_1 & D_2 \\ D_3 & \mu D_4 \end{bmatrix}$$

where D_2, D_3 are $n_2/2 \times n_2/2$ nonsingular matrices and the matrix $D_2 D_3$ has simple and negative eigenvalues $-\omega_i^2$, $i=1,2,\ldots, n_2/2$.

By using the techniques presented in [22-24] it will be shown that in the limit ($\mu \to 0^+$) x_2 can be approximated as a white noise process which can be used as an input to the slow mode x_1. Then the estimation of $x_1(t)$ by ignoring the high frequency oscillations can be analytically represented by the filtering of a reduced order system.

If μ in (A.1b) is neglected and (A.1b) is replaced by

$$0 = A_{21}\bar{x}_1 + A_{22}\bar{x}_2 + B_2\bar{u} + E_2 w$$

then, if A_{22}^{-1} exists,

$$\bar{x}_2 = -A_{22}^{-1} (A_{21}\bar{x}_1 + B_2\bar{u} + E_2 w)$$

and the substitution of $\bar{x}_2$ in (A.1a) results in the reduced order system

$$\dot{\bar{x}}_1 = A_o\bar{x}_1 + B_o\bar{u} + E_o w \qquad (A.3a)$$

$$\bar{y} = C_o\bar{x}_1 + D_o\bar{u} + F_o w + v \qquad (A.3b)$$

where

$$A_o = A_{11} - A_{12}A_{22}^{-1} A_{21}$$

$$B_o = B_1 - A_{12}A_{22}^{-1} B_2$$

$$E_o = E_1 - A_{12}A_{22}^{-1} E_2$$

$$C_o = C_1 - C_2 A_{22}^{-1} A_{21}$$

$$D_o = -C_2 A_{22}^{-1} B_2$$

$$F_o = -C_2 A_{22}^{-1} E_2$$

without any input, the slowly varying part of x_2 is $\bar{x}_2 = -A_{22}^{-1}A_{21}\bar{x}_1$. To separate $\bar{x}_2$ from the highly oscillatory part of x_2, a change of variable is used.

$$\eta = x_2 + A_{22}^{-1} A_{21} x_1 + \mu G x_1 \equiv x_2 + L x_1 \qquad (A.4)$$

transforming (A.1) into

$$\dot{x}_1 = (A_o - \mu A_{12}G)x_1 + A_{12}\eta + B_1 u + E_1 w$$

$$\mu\dot{\eta} = Fx_1 + (A_{22} + \mu L A_{12})\eta + (B_2 + \mu L B_1)u + (E_2 + \mu L E_1)w$$

where

$$F = \mu(A_{22}^{-1} A_{21} + \mu G)(A_o - \mu A_{12}G) - \mu A_{22}G$$

The solution of $F = 0$ is

$$G = A_{22}^{-2} A_{21} A_o + O(\mu)$$

To separate the slow modes, introduce

$$\zeta = x_1 - \mu(A_{12} A_{22}^{-1} + \mu M)\eta \equiv x_1 - \mu H \eta \qquad (A.5)$$

and choose M such that

$$A_{12} + \mu(A_o - \mu A_{12}G)H - H(A_{22} + \mu L A_{12}) = 0$$

so

$$M = A_o A_{12} A_{22}^{-2} - A_{12} A_{22}^{-2} A_{21} A_{12} A_{22}^{-1} + O(\mu)$$

The transformation (A.4) and (A.5) can be written as

$$\begin{bmatrix} \zeta \\ \eta \end{bmatrix} = \begin{bmatrix} I_n - \mu H L & -\mu H \\ L & I_m \end{bmatrix} \begin{bmatrix} x_1 \\ x_2 \end{bmatrix} \qquad (A.6)$$

The original system (A.1) is finally transformed into

$$\dot{\zeta} = A_o \zeta + B_o u + E_o w \qquad (A.7a)$$

$$\mu\dot{\eta} = A_2 \eta + B_2 u + E_2 w \qquad (A.7b)$$

$$y = C_o \zeta + C_2 \eta + v \qquad (A.7c)$$

where

$$A_o = A_o - \mu A_{12}G \simeq A_o + 0(\mu)$$

$$B_o = B_o - \mu(HLB_1 = MB_2) \simeq B_o - 0(\mu)$$

$$E_o = E_o - \mu(HLB_1 + ME_2) \simeq E_o - 0(\mu)$$

$$A_2 = A_{22} + \mu LA_{12} \simeq A_{22} + 0(\mu)$$

$$B_2 = B_2 + \mu LB_1 \simeq B_2 + 0(\mu)$$

$$E_2 = E_2 + \mu LE_1 \simeq E_2 + 0(\mu)$$

$$C_o = C_1 - C_2 L \simeq C_o + 0(\mu)$$

$$C_2 = C_2 + \mu(C_1 - C_2)H \simeq C_2 + 0(\mu)$$

To investigate the behavior of $\eta(t)$, we assume that (A.7b) can be written as

$$\mu \dot{\eta} = A_2 \eta + E_2 w \qquad (A.8)$$

That is, μ has been replaced by the feedback control before applying the transformation to get (A.7)

Let $\tau = \dfrac{t - t_o}{\mu}$, then (A.8) becomes

$$\frac{d}{d\tau} \eta = A_2 \eta + E_2 w$$

where w in the τ- scale has covariance W/μ instead of W in the t-scale. Consequently the covariance of the process $\eta(\tau)$ would also have the form V/μ where V satisfies the eqn.

$$\frac{d}{d\tau} V = A_2 V + V A_2' + E_2 W E_2'$$

with steady state value V satisfying

$$0 = A_2 V_\infty + V_\infty A_2' + E_2 W E_2'$$

If A_2 is stable and given an arbitrary $\epsilon > 0$, then there exists $\mu^* > 0$ and $t_1 > 0$ such that $\|V(t) - V_\infty\| < \epsilon$ for all $t \geqslant t_1$ and $0 < \mu \leqslant \mu^*$. Therefore, for $t > t_1$, $n(t)$ may be approximated by a stationary stochastic process with the autocorrelation function

$$R_\eta(t';t'') = E\{(t')\,(t'')\} = \frac{V_\infty}{\mu} \exp[A_2 \frac{(t'-t'')}{\mu}]\,, \quad t' \leqslant t''$$

However, $R_\eta(t', t'') \rightarrow 0$ as $\mu \rightarrow 0$ for $t' \neq t''$, and

$$\lim_{\mu \rightarrow 0} \int_{t-E}^{t-E} R_\eta(t' - t'')\, dt'' = -A_2^{-1} \bar{V} - \bar{V}A_2'^{-1}$$

where

$$V_\infty = \bar{V} + 0(\mu)$$

so that $\bar{V}$ satisfies

$$A_{22}\bar{V} + \bar{V}A_{22}' + E_2WE_2' = 0$$

It follows that in the limit n becomes a white noise process with covariance

$$\lim_{\mu \rightarrow 0} R_\eta(t', t'') = -(A_{22}^{-1}\bar{V} + \bar{V}A_{22}'^{-1})\,\delta(t' - t'')$$

$$= (A_{22}^{-1}E_2WE_2' A_{22}'^{-1})\,\delta(t' - t'')$$

which is the covariance of the process

$$\bar{n} = A_{22}^{-1}E_2W \simeq A_2^{-1}E_2W$$

obtained by the formal substitution of $\mu = 0$ in (A.8).

The estimation equation for the slow mode is

$$\dot{\hat{\zeta}} = A_o\hat{\zeta} + K_o[\bar{y} - C_o\hat{\zeta}]$$

Since the inverse of (A.6) is

$$
\begin{bmatrix} x_1 \\ x_2 \end{bmatrix} = \begin{bmatrix} I_n & \mu H \\ -L & I_m - \mu LH \end{bmatrix} \begin{bmatrix} \zeta \\ \eta \end{bmatrix}
$$

So the filtered estimate of x_1 and x_2 are given as

$$
\hat{x}_1 = \hat{\zeta} - \mu H \hat{\eta} \simeq \hat{\zeta}
$$

$$
\hat{x}_2 = -L\hat{\zeta} + (I - \mu LH)\hat{\eta}
$$

Since $A_o = A_o + 0(\mu)$, $B_o = B_o + 0(\mu), \ldots$, so

$$
\hat{x}_1 = \hat{\hat{x}}_1 + 0(\mu)
$$

where $\hat{\hat{x}}$ are the estimates obtained by solving the filtering problem for the reduced system (A.3).

VITA

Supat Poopaka

Candidate for the Degree of

Doctor of Philosophy

Thesis: HANDLING QUALITIES OF LARGE FLEXIBLE AIRCRAFT

Major Field: Mechanical Engineering

Biographical:

Personal Data: Born in ███████████████████████
███ the son of Mr. Somboon and Mrs. Pannee Poopaka.

Education: Graduated from Benjamaborpit High School, Bangkok,
Thailand, in 1968; received Bachelor of Science degree
in Mechanical Engineering from Prince of Songkla Univer-
sity, Haadyai, Thailand, in 1972; received Master of
Science degree in Mechanical Engineering from University
of Illinois, Urbana, Illinois, in 1977; completed the re-
quirements for the Doctor of Philosophy degree at Oklahoma
State University in December, 1980.

Professional Experience: Teaching assistant, Mechanical Engi-
neering Department, Prince of Songkla University, 1972-
1975; graduate research assistant, School of Mechanical
and Aerospace Engineering, Oklahoma State University, 1979
to July 1980; King Mongkut Institute of Technology, Bangkok,
Thailand, from 1975 to date (on leave).

End of Document